ON STRUCTURAL RESPONSE OF LARGE LMFBR HEAD CLOSURES TO HYPOTHETICAL CORE DISRUPTIVE ACCIDENTS

R. F. KULAK, T. J. MARCINIAK

Reactor Analysis and Safety Division, Argonne National Laboratory, 9700 South Cass Avenue, Argonne, Illinois 60439, U.S.A.

T. B. BELYTSCHKO

Department of Materials Engineering, University of Illinois at Chicago Circle, Chicago, Illinois 60680, U.S.A.

SUMMARY

One area of concern in the safety evaluation of a pool-type LMFBR head closure is its ability to sustain energetic core disruptive accidents. For the purpose of gaining insight into this important problem this preliminary evaluation of the head closure's capability to withstand a HCDA was undertaken. The overall reactor configuration chosen for the HCDA calculations was based, essentially, upon a scale-up of the Cold-Pool (EBR-II) reactor concept to 1200 Mwe size, but with an integral roof design.

A finite-element model was developed to assess the ability of a pool-type LMFBR head closure to sustain an energetic HCDA. From a conceptual representation of an expanded EBR-II type deck, it was determined that there is a reasonable amount of symmetry in the structure that an initial model would consist of a 12° sector. This model accounts for the main structural elements of the closure head: beams, plates, inner ring, in-tank component nozzle and concrete shielding. The mass of the in-tank component was treated as a concentrated mass located at its attachment to the structural members.

The ANL-developed SADCAT code was used in this study. The code is an explicit, three-dimensional finite-element code developed for analyzing transient, nonlinear, structural problems. The code has a triangular plate element and a three-dimensional continuum element.

The HCDA load applied to the model was in the form of a $p-t$ relationship. This pressure-history was applied to the underside of the bottom annular plate. The pressure-history was derived from the expansion of a 4800°K average temperature core. The initial core volume at the start of the disassembly was taken to be 10.34 m^3. The total energy available in expanding the core to the final quasi-static pressure is about 1400 Mw-sec; if the expansion were continued down to one bar, the total energy available would be about 2720 Mw-sec.

The above model was used to study the effect of several design variations on the structural response of the deck to an energetic HCDA. Two types of outer boundary conditions were considered to determine their effect on the closure head's displacements and stress levels. In addition to the above study, an analysis was conducted to determine the structural contribution of the concrete shielding.

Based upon the above preliminary calculations of pool-type LMFBR head closures, it is indicated that the shield-deck can be designed to survive the given HCDA loads without failure.

1. Introduction

There are essentially two basic system approaches that have been taken in designing Liquid Metal Fast Breeder Reactors (LMFBR); the loop and the pool. In the loop system, which has been the choice for the Fast Test Reactor (FTR) and Clinch River Breeder Reactor (CRBR) in the United States, the reactor cores fuel handling machinery and instrument tree are contained within the primary vessel while the other coolant system components, such as pumps and heat exchangers are connected to it by pipes. The pool-type design, however, has all primary system components enclosed within a comparatively large diameter tank and shield deck.

Among the design features of the pool-type LMFBR system which can have a safety impact are: (1) a highly reliable, simple, low pressure, primary coolant boundary embodied in a single primary tank which enclosed all primary system components; (2) a large primary coolant system heat capacity and reactor inlet and outlet volumes which can provide margins for decay heat removal and protection of components from rapid thermal transients; (3) since in many designs the only piping necessary is a relatively short length between the pump and reactor core inlet, the operating pressures are low, the pipe is isothermal, and there is a low probability of occurrance, as well as severity of consequences, for a loss of piping integrity (LOPI) event, and (4) the large overall cross sectional area of the primary tank can provide for the dissipation of sodium slug impact forces in the event of a Hypothetical Core Disassembly Accident (HCDA) as well as provide for the dispersion of fuel particles resulting from such an event. Based upon these, and other factors, several reactors of the pool-type design are currently operational, under construction, or being designed worldwide. Operational pool LMFBR systems include the Experimental Breeder Reactor-II in the US, the Phenix Reactor (France) and the Prototype Fast Reactor (UK). Currently under construction is the BN-600 (USSR), a 600 Mwe plant, while the French are currently designing a 1200 Mwe plant at Creys-Malville named Super Phenix I. In the UK, a commercial sized LMFBR is also being designed based upon the pool concept.

However, there are some significant problems which must be addressed. Because of the large shield deck necessary to enclose the primary system the question has arisen as to the ability of the deck to resist the forces generated by an energetic HCDA. The purpose of this study has been to address specifically this question in connection to the overall structural design of the deck. The results presented here were part of a study, conducted at Argonne National Laboratory (ANL) for the Energy Research and Development Administration (ERDA), to determine the overall characteristics and concerns of commerical size (∿1200 Mwe) pool-type LMFBR systems [1]. These results are based on a reference reactor system design which was a part of the study and which is used to address the issue from a generic point of view.

II. Reference Reactor Description

Figure 1 is a schematic elevation view of an 1200MWe pool-type reference system. The reactor core region was designed to provide 3000 MW of thermal power with sodium entering at about 700°F and leaving at about 1000°F. The main components of the pool-type LMFBR system are shown: reactor core region, internal heat exchangers (IHXs), primary pumps, core support structure, primary and secondary tanks, and the shield-deck structure. The instrument tree and fuel handling machinery are not shown. Figure 2 shows the plan view of the reference reactor. The primary vessel contains three (3) primary pumps, six (6) IHXs and two (2) storage baskets. The basic dimensions of the pool reactor used in this preliminary study are shown in Fig. 3.

The shield deck itself is an annular structure which is supported by steel columns embedded in the surrounding concrete, radial biological-shield. The major structural components of the deck are the radial I-beams, the bottom annular plate and the inner ring which supports the rotating plugs. The radial beams form a "spoked" type of structure with the central inner ring being the hub. The deck is, in general, a concrete-filled, beam-plate composite structure which provides, in most designs, support for the pumps and heat exchangers, primary and guard tanks, and sufficient radiation shielding.

3. Analytical Methods and Models

Pressure loadings used in this study were obtained from output of the REXCO-HEP [2] containment code. The mathematical model used in the REXCO-HEP calculations is shown in Fig. 3. A description of this model and the assumptions employed is presented below. The reactor region includes representations of the core, axial reflectors and blankets, radial reflectors and blankets, fission-gas plenum, core support structure, and reactor vessel. Between the top of the sodium pool and the bottom of the shield deck and plug structure, there is a cover-gas volume 50.8 cm (20 in.) deep. This gap, of course, is variable from design to design.

Although the plug and shield deck are included in the figure, they were assumed to be rigid in the REXCO calculational model. The plug is shown attached to the shield deck by a set of holddown bolts. Although the REXCO-HEP code would, in general, be capable of calculating the effect that the plug motion has on the shield deck and wall loadings, it was felt to be conservative to ignore this effect for this study. The main tank is assumed to be rigidly attached to the shield deck so that neither axial or radial movement is permitted at this point. From a practical point of view this is a reasonable assumption.

The pressure-volume curve used to describe the core region expansion after an HCDA is shown in Fig. 4. This curve represents an adiabatic expansion of fuel vapor; it has been normalized to the final volume expected in the core expansion which is an input requirement for the REXCO code. The initial core volume (V), at the start of the disassembly was assumed to be $10.34 m^3$. Based on this volume, the V/V_F ratio is 0.0022, where V_F is the final volume of the expanded core. This particular p-v curve is representative of a core with an average temperature of 4800°K at the time of disruption. The total energy available in expanding the core to the final, quasi-static, pressure is about 1400 Mw-sec; if the expansion were continued down to one bar, the total energy available would be about 2720 Mw-sec.

There were several conservatisms inherent in this analysis. These should be mentioned in order to put the following results into proper perspective. The conservatisms were dictated both by time and analytical limitations, but were felt not to affect the general conclusions which could be drawn for the deck structure. Among the conservatisms were (a) the rigid shield deck-and-plug assembly, (b) neglect of internal shrouds, skirts, baffles, and liners, and (c) neglect of pumps, IHXs, instrument trees, and other energy-absorbing structures.

Neglect of the energy-absorbing capability of the deck-and-plug assembly has essentially two effects on the calculational results. The first is that, since the assembly is considered rigid, the loadings during impact are somewhat overestimated. Second, when performing independent, decoupled, calculations on the plug and shield deck, there is again a tendency to overestimate stresses and deflections because of the higher force loadings. Further, the energy absorbed by the plug and shield deck is neglected.

Based on the above model the pressure loading on the deck structure shown in Fig. 5 was obtained. It must be pointed out that the "zero" time shown on Fig. 5 is referred to the beginning of slug impact. Relative to the beginning of the accident, slug impact occurs at about 95msec. The peak pressure was 104 MD/cm^2 and occurred at 9.7msec. The pressure decreases in an oscillatory manner to a quasi-equilibrium pressure at the end of the calculations.

A finite-element computer code SADCAT [3] is the analytical tool used to calculate the shield deck response. SADCAT (Structural Analysis for 3-D Core Assembly Transients) is a computer code developed at ANL for the three-dimensional dynamic or static structural analysis of reactor components. The version used for this study is based upon an explicit, temporal, integration scheme. The code can economically solve large scale, nonlinear (geometric and material) problems. Built-in material laws can model elastoplastic behavior with a multilinear stress-strain curve.

Two types of Finite-elements were used to model the deck structure: a flat triangular plate/shell element and an eight-node, isoparametric hexahedron continuum element.

The shell element is formulated using a co-rotational coordinate system which enables the use of simple strain-nodal displacement and nodal force-stress relations. Plate/shell elements can be subjected to linear in-plane displacements and cubic transverse displacements. The orientation of lumped masses is described by unit vectors, so that arbitrarily large rotations can be treated.

Formulation of the continuum element is done in three-dimensional, Cartesian space, using the tri-linear shape functions described by Zienkiewicz [4]. These shape functions provide continuous, linearly varying, velocity and displacement fields at the element interfaces. The constitutive relations are in a form suitable for a hypoelastoplastic material, that is, the components of the stress rate are linear functions of the components of the rate of deformation. Therefore, the element is applicable to problems characterized by large displacements and large strains.

Using the above code, a finite-element model was designed to assess the ability of a pool-type LMFBR shield-deck to sustain an energetic HCDA. From the plan view of a conceptual representation of an expanded EBR-II type deck, it was determined that there is a reasonable amount of symmetry in the structure, and that an initial model would consist of a 12° sector encompassing one radial I-beam, and one-half of a typical in-tank component (e.g., intermediate heat exchanger, pump, or storage basket). The model is shown in Fig. 6.

The structural components modeled are the main radial I-beam, the component-support I-beam, the inner ring, and the in-tank component nozzles. The model accounts for the mass of the concrete, but ignores its structural effect. The concrete mass is distributed along the main radial I-beam, while the mass of a typical in-tank component is taken into account as a concentrated mass located at its attachment to the radial beam. Although the rotating plug is not modeled explicitly, its mass was taken into account by distributing it along the inner ring. Similarly, the pressure load acting on the plug assembly was treated as a vertical force line load acting on the inner ring of the deck.

A variation of the above model which treats the structural effect of contrete is currently under development.

Type T1 steel was chosen as the material for the radial beams, bottom plate, nozzles, and component support beam. This material combines toughness with a high yield strength and therefore it is well suited for shock type loading. The material properties are listed in Table I. The steel was assumed to follow a bilinear, universal stress-strain curve based upon the mechanical properties listed in Table I. The material properties of the concrete biological shielding are also shown in Table I.

The above models were loaded with the pressure-time curve shown in Fig. 5. This pressure was applied uniformly to the underside of the bottom annular plate. As mentioned above, the plug load was considered to be a line load acting on the inner ring. It was assumed that the in-tank component did not contribute to the loading, except for its mass effect. Also, an investigation of the effect of the inner and outer peripheral boundary conditions on the dynamic behavior of the deck was made using this model in order to assess (a) uncertainties in the design and (b) bounding values for maximum deck deformation.

Results

Once the basic overall dimensions of the deck are determined, the dynamic response of the deck will be influenced by its inner and outer peripheral boundary conditions. For the purpose of ascertaining the effect that different types of boundary conditions have on the dynamic response of the deck the following scoping study was performed. At the outer periphery the head closure is supported by vertical columns which connect directly to the radial I-beams. The beams and columns were considered to be connected by either a bolted joint or a welded, stiffened corner. The bolted joint corresponds to a "pinned" type of boundary connection and the welded corner corresponds to a "fixed-end" boundary condition.

At the deck's inner periphery the choice of the boundary condition is not as obvious. Here the boundary condition is determined by the manner in which the rotating-plug assembly is connected to the deck. The rotating-plug assembly would be connected to the top area of the inner ring with a substantial holddown bolting system. Because of this holddown system and the large stiffness of the plug assembly, it is believed that there would be little radial differential movement between the plug assembly and the deck at the top of the inner ring. Therefore, it was assumed that the top of the inner ring can move vertically and that it is restricted from radial motion. This boundary condition corresponds to a "pinned-end" condition in which vertical motion is permitted. The remainder of the inner ring is separated from the plug assembly by a relatively small clearance gap. Depending on the size of this gap, the plug assembly may further restrict the inner ring from rotating during loading. This motion constraint would occur when the gap dimension is small. In contrast, if the gap is relatively large no restrain would occur.

An assessment of this constraint condition on the dynamic response of the deck was made by considering the following two types of boundary conditions. The small gap design was modelled by preventing the entire inner ring from rotating. Thus for this condition the movement of the entire inner ring is restricted to vertical motion. When the gap dimension is large the plug assembly would not put any rotational restriction on the inner ring and the ring can rotate but would be restricted from radial motion at its top due to the previously discussed holddown bolting system. Table II identifies the various boundary condition combinations studies and also relates them to a case number.

The vertical displacements of the radial I-beam at its connection to the inner ring is shown in Fig. 7 for the various boundary condition combinations. It is seen that the end conditions strongly influence the displacement magnitudes as well as the peak displacement times. The largest peak displacements occurred for case B which was the constrained inner ring and the pinned-end beam column joint; the smallest displacement for case A which was the constrained inner ring and the fixed-ended radial beam. It was noted that the largest peak displacement (case B) was three times the smallest (case A). Table III summarized the peak displacements and the time after slug impact at which they occur. From Fig. 7 it is seen that for case A and B, both of which have a fixed inner ring, the initial displacements are nearly identical for the first 18 msec after slug impact and thereafter they differ markedly. A comparison between cases A and C, which differ only in the inner ring support connection, shows that the simply-supported inner ring model initially deflects more than the fixed-supported model. Therefore, it appears that the initial displacements are governed to a certain extent by the inner-ring support connection and that the maximum displacement is influenced by both the inner-ring and radial I-beam support methods. Thus the choice of the support connections for the deck are important considerations in the design of the deck.

The following is a description of the deck's energy partitioning for the case of a pinned inner ring and a fixed-end radial beam. At slug impact, some of the axial kinetic energy of the sodium is transferred to strain and kinetic energy in the deck. The deck's kinetic energy and strain energy histories are shown in Fig. 8. The kinetic energy reaches a peak value of 21 MJ at 0.0142 sec after slug impact and then decreases to a small value. The strain energy peaks out at a level of 76 MJ at 0.035 sec after slug impact. In Ref. 1, it was reported that the maximum main tank strain energy for this reactor configuration was 1114 MJ. Therefore, it is seen that the strain energy of the deck is about one-fifteenth that of the main tank.

Summary and Conclusions

A preliminary study of the dynamic response of a large (1200 MWe) pool-type deck structure to an energetic core dissassembly accident was performed. The analysis proceeded as two independent, decoupled calculations: containment calculations and deck response calculations. The containment calculations were performed mainly to derive a loading pressure history for the deck structure. In this part of the study, the deck was considered rigid so the derived loading pressures were conservative.

In the second part of the study a set of independent deck response calculations were performed using the above derived loading pressure history as input. A finite-element model that incorporated the main structural components of the deck was constructed. A preliminary study of the dynamic response of the deck was performed using this model. Also, the effect that different types of boundary conditions have on the dynamic response of the deck was studied.

Based on the above preliminary studies, it is concludedthat the deck structure can maintain its structural integrity under the given energy release.

Acknowledgments

The authors wish to thank Dr. S. H. Fistedis for his guidance and support during the performance of this work and to Mr. C. Fiala for his programming assistance. This work was performed in the Engineering Mechanics Section of the Reactor Analysis and Safety Division at Argonne National Laboratory under the auspices of the U.S. Energy Research and Development Administration.

References

[1] Amorosi, A., Hutter, E., Marciniak, T. J., Monson, H. O., Seidensticker, R. W., and Simmons, W. R., An Overview of Pool-Type LMFBRs: General Characteristics, ANL-76-61 (May 1976).

[2] Chang, Y. W., and Gvildys, J., REXCO-HEP: A Two-dimensional Computer Code for Calculating the Primary System Response in Fast Reactors, ANL-75-19 (June 1975).

[3] Marchertas, A. H. and Belytschko, t. B., Nonlinear Finite-Element Formulation for Transient Analysis of Three-Dimensional Thin Structures, ANL-8104 (June 1974).

[4] Zienkiewicz, O. C., "The Finite Element Method in Engineering Science," McGraw-Hill, London, (1971).

TABLE I. MATERIAL PROPERTIES

	T1 Steel	Concrete
Youngs Modulus	206 GPa	28 GPa
Poisson's Ratio	0.3	0.18
Yield Stress	620 MPa	--
Ultimate Stress	724 MPa	--
Tangent Modulus	620 MPa	--

TABLE II. DECK BOUNDARY CONDITIONS

Case	Inner	Outer
A	Fixed	Fixed
B	Fixed	Pinned
C	Pinned	Fixed

TABLE III. PEAK VERTICAL DISPLACEMENTS

Case	Displacement (cm)	Time (msec)
A	4.17	25
B	9.37	50
C	7.54	36

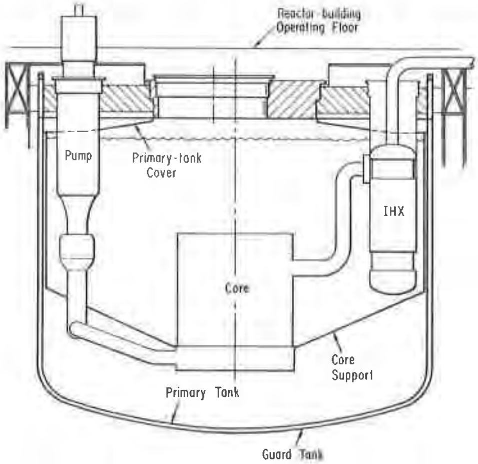

1. Schematic Elevation View of Pool-Type LMFBR Based on Cold-Pool (EBR-II) Design

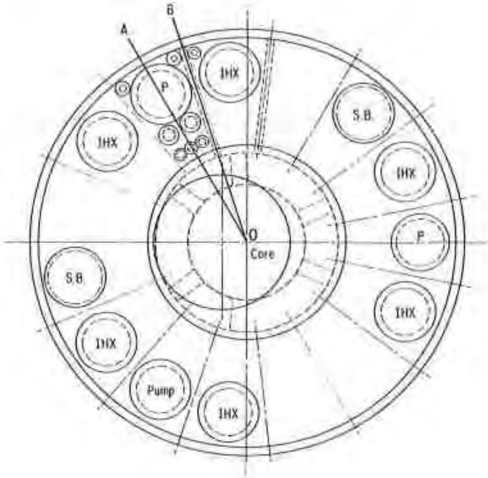

2. Schematic Plan View of Pool-Type LMFBR

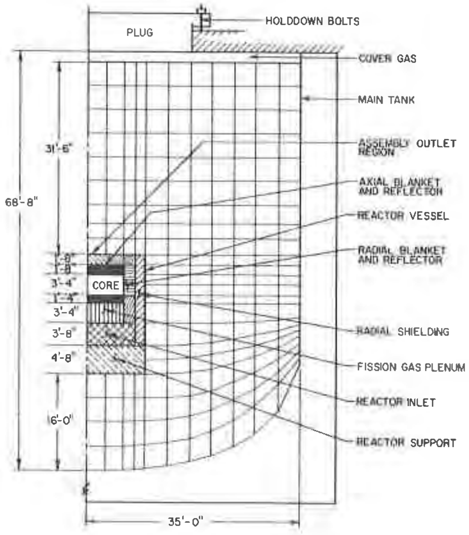

3. Mathematical Model of Reference Reac for Containment Calculations

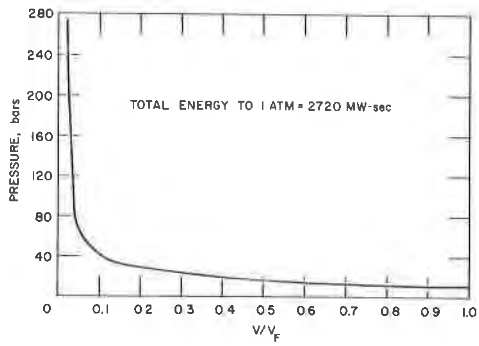

4. Normalized Core Pressure-Volume Curve for 4800°K Average Core Temperature

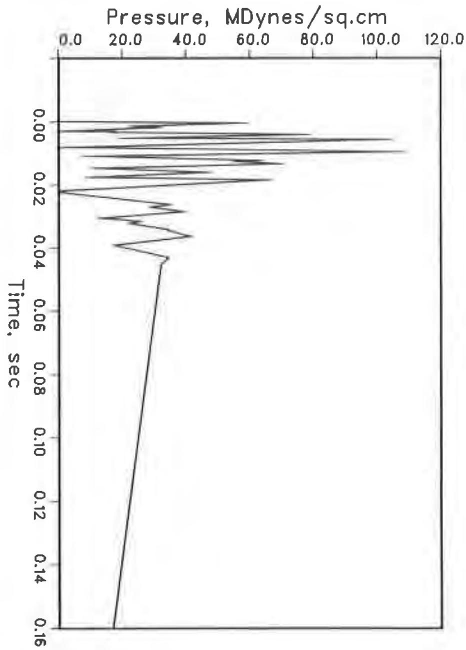

5. **Pressure-Time Loading of Shield-Deck Due to an HCDA**

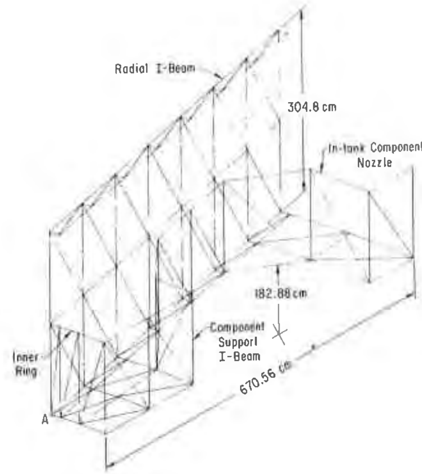

6. **Finite-Element Model of 12° Shield-Deck Segment Used for Deck Response Calculations**

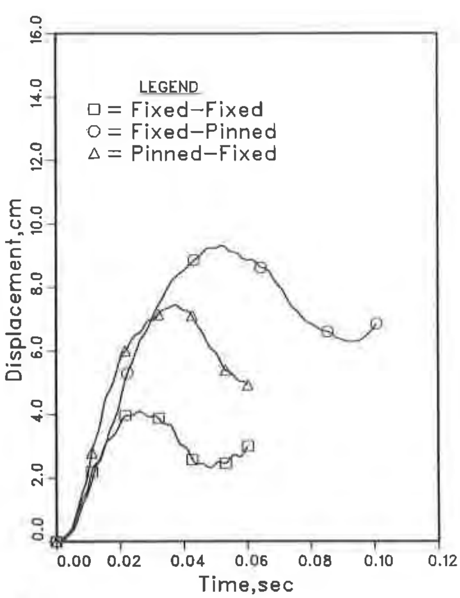

7. **Vertical Displacement Histories of the Radial I-Beam at Its Connection to the Inner Ring**

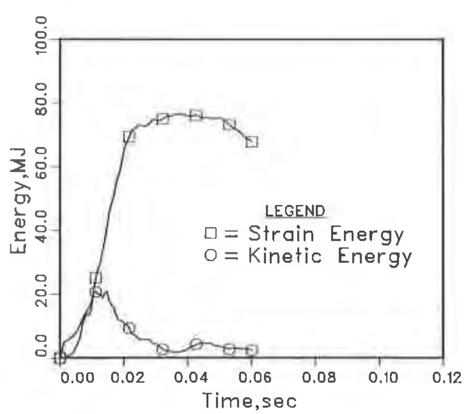

8. **Kinetic and Strain Energies of the Shield Deck for the Case of a "Pinned" Inner Ring Connection and a Fixed-End Radial Beam/Column Joint**